Coupling of surface roughness to the performance of computer-generated holograms

Ping Zhou* and Jim Burge

College of Optical Sciences, University of Arizona, Tucson, Arizona 85721, USA

*Corresponding author: pzhou@optics.arizona.edu

Received 23 April 2007; accepted 3 July 2007;
posted 5 July 2007 (Doc. ID 82325); published 5 September 2007

Computer-generated holograms (CGHs), such as those used in optical testing, are created by etching patterns into an optical substrate. Imperfections in the etching can cause small scale surface roughness that varies across the pattern. The variation in this roughness affects the phase and amplitude of the wavefronts in the various diffraction orders. A simplified model is developed and validated that treats the scattering loss from the roughness as an amplitude effect. We demonstrate the use of this model for engineering analysis and provide a graphical method for understanding the application. Furthermore, we investigate the magnitude of this effect for the application of optical testing and show that the effect on measurement accuracy is limited to 1 nm for typical CGHs.

OCIS codes: 050.1380, 050.2770.

1. Introduction

Computer-generated holograms (CGHs) play an important role in a variety of applications in modern optics. Such applications include beam shaping, image processing, and optical testing [1]. The pattern on a CGH determines whether the wavefront is split into a number of beams, compensates for some aberrations in an optical assembly, or performs other useful optical functions. This high degree of flexibility in creating complex wavefronts has made CGHs extremely useful. A properly designed CGH can perform the functions of a conventional lens or mirror. They also have the potential to be thin, lightweight, and cost effective. CGHs have been most successful for optical testing of aspheric surfaces, where the CGH can be used to control the shape of a highly aspheric wavefront to less than a hundredth of a wave [2].

Errors in the CGH fabrication can cause the diffracted wavefront to suffer aberrations. Manufacturing limitations result in errors in the pattern distortion, linewidth, etching depth, and surface roughness. The first three fabrication errors have been studied by Chang and Burge [3,4]. In this paper, the coupling of surface roughness to the wavefront phase and diffraction efficiency is discussed. A parametric model is built to analyze the coupling of surface roughness to performance based on the scalar diffraction theory. A computer simulation of the effects of surface roughness is provided in Section 3. The coupling of surface roughness variation to wavefront errors is developed in Section 4. A simple graphical representation is introduced to further explain the coupling of surface roughness to diffraction efficiency and wavefront phase.

2. Parametric Model

A binary, linear grating model is used to build the parametric model because many complicated CGHs can be viewed as a collection of binary, linear gratings with various spatial frequencies. The grating is specified by the period S, the width of the etched area b, and the etching depth t. Duty cycle is defined as $D = b/S$. A_0 and A_1 are the amplitudes of the output wavefront from the unetched and etched area of the grating, respectively. The values of A_0 and A_1 can be determined by the reflectance or the transmittance coefficients at the grating interface. The phase function ϕ represents the phase difference between rays from the peaks and the valleys of the grating structure, which is equal to $2\pi(n-1)t/\lambda$ for the grating in transmission, where n is the refractive index of the grating.

0003-6935/07/266572-05$15.00/0

Table 1. Summary of Diffraction Efficiencies and Wavefront Phases

	Zero Order ($m = 0$)	Nonzero Order ($m \pm 1, \pm 2, \ldots$)
η	$A_0^2(1-D)^2 + A_1^2D^2 + 2A_0A_1D(1-D)\cos(\phi)$	$[A_0^2 + A_1^2 - 2A_0A_1\cos(\phi)]D^2\,\mathrm{sinc}^2(mD)$
$\tan(\Psi)$	$\dfrac{A_1D\sin(\phi)}{A_0(1-D)+A_1D\cos(\phi)}$	$\dfrac{A_1\sin(\phi)\mathrm{sinc}(mD)}{[-A_0+A_1\cos(\phi)]\mathrm{sinc}(mD)}$

Assuming that the grating above is illuminated by a planar wavefront at normal incidence, the output wavefront immediately past the grating, either reflected or transmitted, can be expressed as

$$u(x) = A_0 + (A_1e^{i\phi} - A_0)\mathrm{rect}\left(\frac{x}{b}\right) * \frac{1}{S}\,\mathrm{comb}\left(\frac{x}{S}\right). \tag{1}$$

Based on Fraunhofer diffraction theory, the far-field diffraction wavefront can be obtained by taking the Fourier transform of this output wavefront, which is

$$U(\xi) = \begin{cases} \{A_0 + [A_1\cos(\phi) - A_0]D\} + i\{A_1\sin(\phi)D\} & m = 0 \\ \{[A_1\cos(\phi) - A_0]D\,\mathrm{sinc}(mD)\} + i\{A_1\sin(\phi)D\,\mathrm{sinc}(mD)\} & m = \pm 1,\ \pm 2, \ldots, \end{cases} \tag{2}$$

where ξ gives the component of the diffracted light at the angle $m\lambda/S$. Assuming the intensity of the incident wavefront is unity, the diffraction efficiency is the modulus squared of the complex wavefront, and the wavefront phase is the inverse tangent of the ratio of the real and imaginary parts of the complex wavefront. Table 1 lists the diffraction efficiencies η and wavefront phase Ψ for the zero and the nonzero diffraction orders in the far-field regime. The equation indicates that the wavefront phase is not affected by duty cycle for nonzero diffraction orders. The reason that the $\mathrm{sinc}(mD)$ functions are left in both the numerator and the denominator is to preserve the sign information for the wavefront phase.

A real grating is not as perfect as shown in Fig. 1. Both the top and the bottom surfaces have roughness, especially after reactive ion etching is used to create the structures [5]. The rms roughness between the top and bottom (etched) surfaces may vary from several angstroms to several nanometers, depending on the techniques of etching. Figure 2 shows a simulated grating profile. For simplicity, only the bottom surface is shown with roughness. The local etching depth can be defined as the average phase difference between the top surface and the bottom surface. If the surface roughness is on a scale that is much smaller than the period of the pattern, the coupling of the scattered light into the diffracted light can be ignored, since the light is scattered at wide angles. However, the values of A_0 and A_1 are reduced due to scattering, and the scattered light itself may cause ghost or glare in the optical system.

It is hard to measure the scattering losses of a CGH directly. One useful method is to measure the surface roughness, and then calculate the scattering using the total integrated scatter (TIS) formula. The surface roughness can be measured by an interference microscope [6].

The TIS formula relates the surface rms roughness to the scattered light by comparing the amount of light that is reflected specularly from a surface to the amount of light that is reflected diffusely. The TIS in reflection TIS_r can be calculated by

$$\mathrm{TIS}_r = \frac{I_{\mathrm{scat}}}{I_{\mathrm{ref}}} = (2\pi\sigma)^2 = \left(\frac{4\pi}{\lambda}R_q\right)^2. \tag{3}$$

A similar formula to calculate the TIS for the transmitted light TIS_t:

$$\mathrm{TIS}_t = \frac{I_{\mathrm{scat}}}{I_{\mathrm{trans}}} = (2\pi\sigma)^2 = [2\pi(n-1)R_q/\lambda]^2, \tag{4}$$

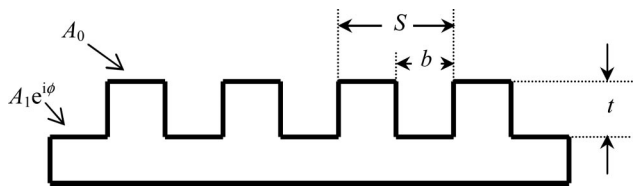

Fig. 1. Illustrates an ideal binary, linear grating.

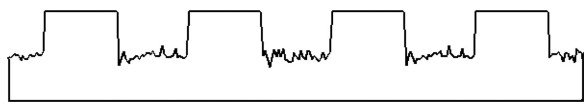
Fig. 2. Actual profile of a binary, linear grating.

where σ is the wavefront standard deviation in units of waves, n is the index of refraction of the grating substrate, and R_q is the surface rms roughness. The amplitude of the output wavefront after the rough surface can be determined by

$$A = A_{\text{Fresnel}}\sqrt{1 - \text{TIS}}, \tag{5}$$

where A_{Fresnel} is the amplitude of transmitted or reflected light due to the Fresnel effect if there is no scattering. The product of A_{Fresnel} and a small correction $\sqrt{1-\text{TIS}}$ gives the effective amplitude that can be applied to calculate the diffraction efficiency and wavefront phase. Therefore, the problem of surface roughness can be simply treated as a light loss from the rough surface. The wavefront phase and diffraction efficiency can be calculated by using the scatter-corrected amplitudes. If both the top surface and bottom surface are rough, the scattered loss from both surfaces has to be considered, which means both A_0 and A_1 need to be modified.

The surface roughness varies across the substrate due to limitations in the etching process. The variation of surface roughness can cause light to scatter differently at various locations across the grating. The variation in amplitude causes wavefront errors and nonuniformity in diffraction efficiency. In Section 3 the performance of a binary, linear grating with a rough surface is simulated to demonstrate how scattering affects the wavefront phase and diffraction efficiency.

3. Numerical Demonstration

An example of a binary, linear, phase grating is used to illustrate the coupling of the surface roughness to its performance. A random surface height error with a Gaussian distribution is added to the bottom surface in each period, assuming the top surface is perfectly smooth. Since we are interested in the coupling of roughness *variation* across the substrate, we model a grating that has a sinusoid distribution across the grating, so the bottom surface is rougher at the center and smoother at the edges. The duty cycle and etching depth of this grating are 50% and 0.35λ, respectively. The amplitudes A_0 and A_1 are unity if there is no scattered loss. Therefore, this rough grating is equivalent to a grating with a constant phase ϕ, duty cycle D, amplitude A_0, and varying amplitude A_1. The actual grating relief and its equivalent model are illustrated in Fig. 3.

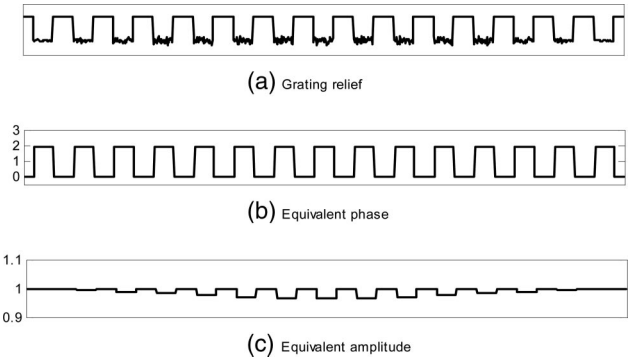

Fig. 3. Rough grating and its equivalent model.

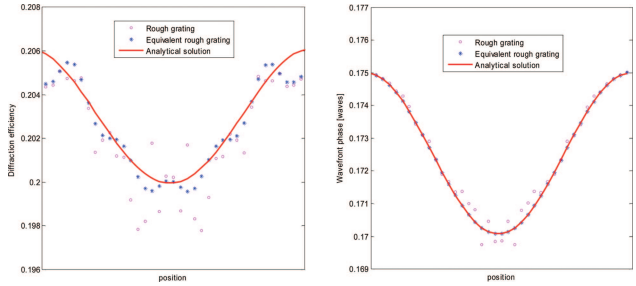

Fig. 4. (Color online) Zero-order diffraction efficiency and wavefront phase across the grating (50% duty cycle and 0.35λ etching depth).

The roughness of the bottom surface over the grating ranges from 0 to 0.08λ rms. Assuming the refractive index of the grating is 1.5, and the grating is used in transmission, the equivalent amplitude A_1 varies from 1 to 0.968 using Eq. (5). The *P-V* amplitude variation is 0.032, and the rms amplitude variation is 0.011. This equivalent model allows rapid calculation of the effects of scatter, and provides some physical insight to the behavior.

To simulate the far-field diffraction, we first take a Fourier transform of the output wavefront right after the grating for both the actual grating with the roughness and its equivalent model, which treats only the amplitude effects of the scatter. After propagating the wavefronts, a spatial filter is used to select a desired diffraction order. Finally, an inverse Fourier transform is applied to obtain the complex wavefront in the far field for that particular order.

The simulation results are shown in Figs. 4 and 5. The circle markers represent the actual grating with the rough bottom surfaces as shown in Fig. 3(a). The asterisk markers represent the equivalent model, and the solid curves represent the analytical solution using the equations from Table 1. At different locations of the grating, different values of A_1 are used in the equations to calculate the wavefront phase and diffraction efficiencies. A local averaging filter is used on all the curves to smooth the data. From the simulation results, we can see that the equivalent model matches both the rough grating and

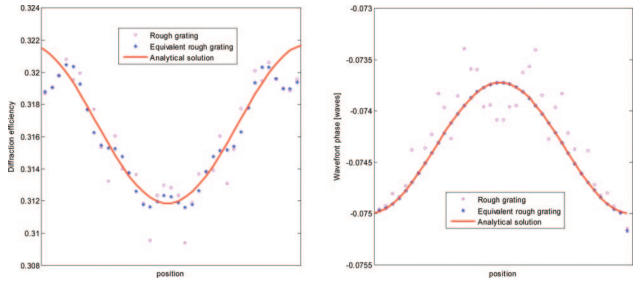

Fig. 5. (Color online) First-order diffraction efficiency and wavefront phase across the grating (50% duty cycle and 0.35λ etching depth).

Table 2. Sensitivity Functions for Diffraction Efficiencies and Wavefront Phases

	Zero Order ($m = 0$)	Nonzero Order ($m \pm 1, \pm 2, \ldots$)
$\frac{\partial \eta}{\partial A_1}$	$2A_1D^2 + 2A_0D(1 - D)\cos(\phi)$	$(2A_1 - 2A_0\cos(\phi))D^2\,\mathrm{sinc}^2(mD)$
$\frac{\partial \Psi}{\partial A_1}$	$\frac{A_0D(1-D)\sin(\phi)}{A_0^2(1-D)^2 + A_1^2D^2 + 2A_0A_1D(1-D)\cos(\phi)}$	$\frac{-A_0\sin(\phi)}{A_0^2 + A_1^2 - 2A_0A_1\cos(\phi)}$

analytical calculation. The rough grating has random noise, because the spatial filter has a finite size that allows some lower-order scattering to come into the optical system.

The simulation shows that with 50% duty cycle and 0.35λ etching depth, the diffraction efficiencies decrease with an increase in the surface roughness for both the zero and the first diffraction orders, while the effects of surface roughness on the wavefront phase are opposite. The surface roughness causes the wavefront phase to decrease in the zero diffraction order and increase in the first order.

The numerical model demonstrates that the small scale surface roughness can be treated purely as an amplitude effect. Rather than treating the roughness directly, we can measure the surface roughness of the grating and treat it as the scattering loss.

4. Errors Analysis due to Surface Roughness

When applying CGHs in any application, it is necessary to evaluate them in order to assure the accuracy and validity of the measurement results. The coupling of surface roughness to the performance on diffraction efficiency and wavefront phase can be obtained by measuring the surface roughness variation over the sampled points of CGHs and converting it to the amplitude variation. The variation in diffraction efficiency and wavefront phase caused by the surface roughness can be evaluated by

$$\Delta\eta_{A_1} = \frac{\partial \eta}{\partial A_1}\,\Delta A_1, \tag{6}$$

$$\Delta W_{A_1} = \frac{1}{2\pi}\,\frac{\partial \Psi}{\partial A_1}\,\Delta A_1, \tag{7}$$

where ΔW_{A_1} is the wavefront variation in waves due to surface roughness, $\Delta\eta_{A_1}$ is the diffraction efficiency variation due to surface roughness, and ΔA_1 is the variation in amplitude due to scattering, using the equivalent model.

$\partial\eta/\partial A_1$ and $\partial\Psi/\partial A_1$ are the derivative of diffraction efficiency and wavefront phase with respect to A_1, which are called as the "sensitivity functions." The sensitivity functions can be evaluated directly to give the wavefront error and efficiency error for a given surface roughness variation. Table 2 shows the sensitivity functions for amplitude A_1. It can be expanded for both amplitude A_0 and amplitude A_1, if the surface roughness of the top surface needs to be taken into account.

As long as the surface roughness varies over spatial scales that are large compared to the grating spacing, the sensitivity functions can be used to determine the coupling between the surface roughness variation and system performance. Figure 6 shows the diffraction efficiency sensitivities to the amplitude A_1 at various duty cycles for both the zero order and the first order, assuming it is a phase grating with the nominal values of A_1 and A_0 unity. The point with 50% duty cycle and 0.35λ etching depth, which are the parameters of the CGH used in Section 3, is marked as an asterisk in the figure. At that point, the diffraction efficiency sensitivities of amplitude for the zero order and the first order are 0.206 and 0.322, respectively, where the units are (diffraction efficiency variation)/(variation in amplitude).

Similarly, wavefront phase sensitivity functions for both the zero order and the first order are shown in Fig. 7. The wavefront sensitivity functions for the first order are the same for all the duty cycles, which indicates that the wavefront phase is not sensitive to the duty cycle. This phenomenon has been predicted by the wavefront phase function in Table 1. At 50% duty cycle and 0.35λ etching depth, the phase sensi-

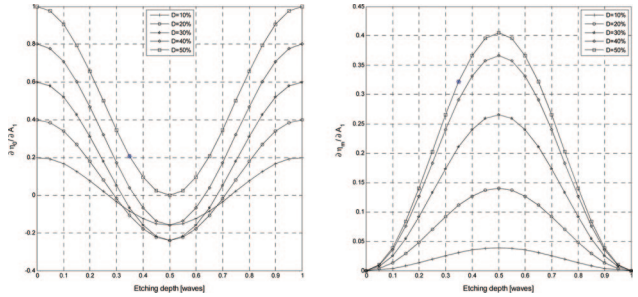

Fig. 6. (Color online) Diffraction efficiency sensitivity for the (left) zero order and the (right) first order.

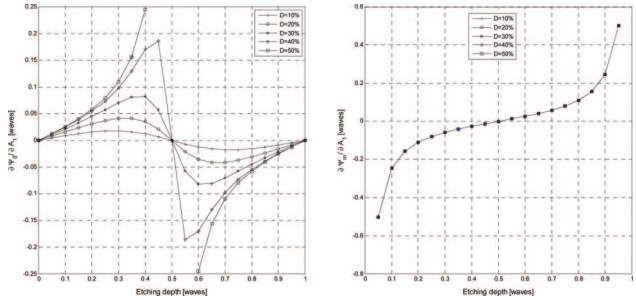

Fig. 7. (Color online) Wavefront phase sensitivity for the (left) zero order and the (right) first order.

Table 3. Diffraction Efficiency Variation and Wavefront Phase Variation From Surface Roughness (50% Duty Cycle and 0.35λ Etching Depth)

	Sensitivities	*P-V* Error	rms Error
Diffraction efficiency			
Zero order	0.206	0.0064	0.0023
First order	0.322	0.0100	0.0035
Wavefront phase			
Zero order	0.156λ	0.0048λ	0.0017λ
First order	−0.041λ	−0.0013λ	−0.0005λ

tivities for zero order and first order are 0.156λ and −0.041λ, respectively, where the units are (wavefront phase variation in waves)/(variation in amplitude).

Variations in diffraction efficiency and wavefront phase can be computed by applying the sensitivity functions with the amplitude variation, which is due to the variation in surface roughness. For the case we demonstrated in Section 3, the *P-V* amplitude variation is 0.032, and the rms amplitude variation is 0.011. The *P-V* and rms variation in diffraction efficiency and wavefront phase are listed in Table 3. The *P-V* variations match the computer simulation results in Section 3.

Note that surface roughness can be ignored if the CGH is small, since the surface roughness may be sufficiently uniform in a small scale. For a large-scale CGH, nonuniformity in surface roughness will become an issue. The variation in surface roughness will cause the variation in diffraction efficiency and wavefront phase.

The wavefront error of a 5 in. (127 mm) diameter phase CGH was calculated using measured surface roughness, taken with an interference microscope. The surface roughness was found to be 2 nm ± 0.5 nm rms. The scattered loss was 0.01% ± 0.005%, and the amplitude variation was 0.005%. Therefore, the coupling of the surface roughness to the wavefront phase was less than 1 nm, which is small enough to be ignored.

5. Graphical Representation of Diffraction Field

The coupling of surface roughness to performance can also be examined by plotting the real and imaginary part of the complex field in a complex coordinate system. The complex wavefront is for a binary, linear grating is derived in Eq. (2). Both diffraction efficiency and wavefront phase values may be easily obtained from the plot. Figure 8 gives a demonstration of this graphical representation. The circles in the plot contain the complete solutions of a phase grating with 50% duty cycle. The difference between the two circles in each plot is the amplitude. Each point in the circle corresponds to different values of etching depth. A vector pointing from the origin of the complex coordinate to a point on the circle corresponds to a solution of the diffraction fields produced by the grating at a specific etching depth. The magnitude of the vector gives the amplitude of the diffraction field, while the angle between the vector and the real axis gives the wavefront phase value Ψ of the diffraction field.

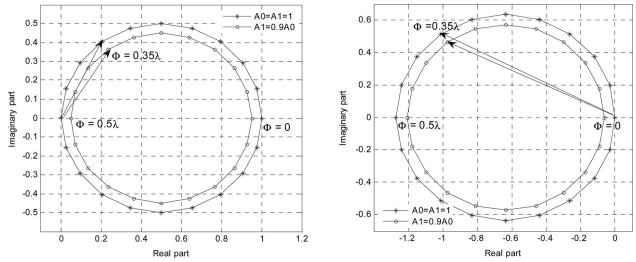

Fig. 8. Graphical representation for (left) zero- and (right) first-order diffraction.

In Fig. 8, all the vectors are pointing to the $\phi = 0.35\lambda$ on the circle. In each figure, one circle represents the case without scattering, which means $A_1 = A_0 = 1$. The other circle represents the case with scattering, where $A_1 = 0.9A_0$. The scattering causes the circle to shrink towards its center. For zero-order diffraction, the scattering decreases the wavefront phase, while it causes an increase in the wavefront phase for the first order. While the diffraction efficiency decreases in both cases, it drops more for the first order.

As we can see, the graphical representation provides an intuitive view of the diffracted wavefront. It helps to understand how the wavefront phase and diffraction efficiency change with duty cycle, etching depth, and amplitude.

6. Conclusion

The effect of surface roughness on a computer-generated hologram (CGH) was analyzed based on Fraunhofer diffraction theory. The numerical simulation showed that fabrication tolerances on surface roughness can result in variations in diffraction efficiency and wavefront phase. Sensitivity functions due to amplitude variations were derived, and they helped to estimate the impact of surface roughness on the diffraction efficiency and wavefront phase of a sample CGH. For typical CGHs used in optical testing, the effect of the surface roughness on measurement accuracy can be ignored. A simple graphical model of diffraction field was also found to be useful in showing the relationship between surface roughness and performance.

References

1. T. K. Gaylord and M. G. Moharam, "Analysis and applications of optical diffraction by gratings," Proc. IEEE **73,** 894–937 (1985).
2. P. Zhou and J. H. Burge, "Fabrication error analysis and experimental demonstration for computer-generated holograms," Appl. Opt. **46,** (2007).
3. Y. C. Chang and J. H. Burge, "Errors analysis for CGH optical testing," Proc. SPIE **3782,** 358–366 (1999).
4. Y. C. Chang, P. Zhou, and J. H. Burge, "Analysis of phase sensitivity for binary computer generated holograms," Appl. Opt. **45,** 4223–4234 (2006).
5. D. W. Ricks and L. V. Chizek, "Light scattering from binary optics," Proc. SPIE **1211,** 24–37 (1990).
6. C. Saxer and K. Freischlad, "Interference microscope for sub-Angstrom surface roughness measurement," Proc. SPIE **5144,** 37–45 (2003).